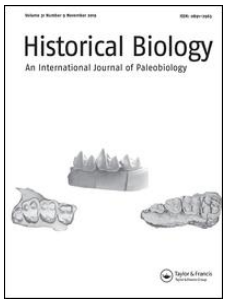

Historical Biology

An International Journal of Paleobiology

ISSN: (Print) (Online) Journal homepage: https://www.tandfonline.com/loi/ghbi20

A Late Pleistocene third molar of *Hylochoerus* (Suidae, Mammalia) from Rusinga Island, Kenya: paleoenvironmental implications and a note on the hypsodonty of African forest hogs

Ignacio A. Lazagabaster, Thure E. Cerling & J. Tyler Faith

To cite this article: Ignacio A. Lazagabaster, Thure E. Cerling & J. Tyler Faith (2021): A Late Pleistocene third molar of *Hylochoerus* (Suidae, Mammalia) from Rusinga Island, Kenya: paleoenvironmental implications and a note on the hypsodonty of African forest hogs, Historical Biology, DOI: 10.1080/08912963.2021.1887861

To link to this article: https://doi.org/10.1080/08912963.2021.1887861

HISTORICAL BIOLOGY
https://doi.org/10.1080/08912963.2021.1887861

Taylor & Francis
Taylor & Francis Group

ARTICLE

A Late Pleistocene third molar of *Hylochoerus* (Suidae, Mammalia) from Rusinga Island, Kenya: paleoenvironmental implications and a note on the hypsodonty of African forest hogs

Ignacio A. Lazagabaster [a,b], Thure E. Cerling [c] and J. Tyler Faith [d,e]

[a]Leibniz Institute for Research on Evolution and Biodiversity, Museum Für Naturkunde, Berlin, Germany; [b]Department of Maritime Civilizations, Charney School of Marine Science and Recanati Institute for Maritime Studies, University of Haifa, Haifa, Israel; [c]Department of Geology and Geophysics, University of Utah, Salt Lake City, UT, USA; [d]Natural History Museum of Utah, University of Utah, Salt Lake City, Utah, USA; [e]Department of Anthropology, University of Utah, Salt Lake City, UT, USA

ABSTRACT

African forest hogs (genus *Hylochoerus*) are extant Afro-tropical suids that inhabit a variety of forest environments and thick bushlands and are predominantly herbivores. *Hylochoerus* likely evolved from a Pleistocene *Kolpochoerus majus*-like ancestor, but its recent evolutionary history is virtually unknown. Here, we describe a partial right lower third molar from the Late Pleistocene Wasiriya Beds of Rusinga Island (~50-36 ka). The crowns are mesiodistally compressed in a bunolophodont fashion and arranged in columnar pillars that resemble those of extant *Hylochoerus*. We provide accurate data derived from computed tomography on the hypsodonty index (HI) of extant *Hylochoerus* and show that the Rusinga third molar crown was as tall as those of its modern counterpart (HI = 1.8–2.0). Stable carbon isotope analyses suggest that the diet of the Rusinga specimen ($\delta^{13}C$ = −17.0 ‰) was also like that of extant forest hogs ($\delta^{13}C$ average = −17.6 ‰). This extremely negative value contrasts strikingly with those of other fossil large herbivores at Rusinga ($\delta^{13}C$ average = −0.7 ‰.). Among the potential explanations for this anomaly, the most likely is that the Late Pleistocene paleoenvironments were more heterogeneous than previously considered and may have included closed-canopy woodland in the highlands of Rusinga.

ARTICLE HISTORY
Received 18 November 2020
Accepted 4 February 2021

KEYWORDS
Fossil; stable isotopes; ecology; third molar; computed tomography

Introduction

Despite the rich eastern African Plio-Pleistocene fossil record, the latest part of the Pleistocene is not well sampled, and the fossil record tends to be sparse. As a result, the recent evolutionary history of many African taxa remains obscured (Frantz et al. 2016). Today, sub-Saharan African Suidae form a clade with three genera, *Potamochoerus, Phacochoerus*, and *Hylochoerus*, all of which show distinct craniomandibular and dental adaptations and diverse ecological associations (Ewer 1958, 1970; Harris and White 1979; Harris and Cerling 2002; Souron 2012, 2017; Souron et al. 2015a; Lazagabaster 2019). The two living *Potamochoerus* species retain a relatively primitive suine dentition, characterised by low-crowned, bunodont teeth with thick enamel. Extant *Potamochoerus* species show a high degree of dietary flexibility, being capable of exploiting a wide array of dietary items throughout different habitats, from closed forest to open woodland/bushland (Leus and Macdonald 1997; Melletti et al. 2017; Seydack 2017). The craniomandibular and dental similarities of *Potamochoerus* with Pliocene *Kolpochoerus* and other archaic-looking specimens have brought confusion to the origin and evolution of these genera (White 1995; Bishop 2010; Souron 2012; Souron et al. J-R 2015b). Warthogs (genus *Phacochoerus*) have high-crowned third molars arranged in multiple rows of rounded columnar pillars. Their hypsodont dentition allows them to feed on grasses for most of the year in various types of open and occasionally dry savannah grassland/bushland habitats (Cumming 1975, 2013; Butynski and Jong 2017). *Phacochoerus* likely descends from a stock of Plio-Pleistocene *Metridiochoerus* via *M. modestus* but the early divergence of the two living warthog species inferred from molecular studies is strongly at odds with the fossil record because warthogs older than 1.5–1.0 Ma are unknown (Harris and White 1979; Gongora et al. 2011; Frantz et al. 2016).

African forest hogs are the largest on average of all the wild suids on Earth, though some wild boar populations and domestic pigs can be larger (D'Huart 1993; D'Huart and Kingdon 2013; Reyna-Hurtado et al. 2017). Only one species in the genus *Hylochoerus* has traditionally been recognised, *H. meinertzhageni*, with at least three subspecies accepted (Grubb 1993, 2005; D'Huart and Kingdon 2013), but it has been suggested that these forms could represent three different species (Groves and Grubb 2011; Gongora et al. 2017). The diet of forest hogs consists mainly of herbaceous plants and grasses (D'Huart and Kingdon 2013; Reyna-Hurtado et al. 2017), and they also feed occasionally on woody plants, ferns, seeds, larvae, worms, carrion, and eggs (D'Huart 1978; Kingdon 1979). Forest hogs mostly occupy Afrotropical montane forests and other closed habitats throughout western, central, and eastern Africa (Figure 1, D'Huart 1993, Cerling and Viehl 2004, D'Huart and Kingdon 2013, D'Huart and Yohannes 2014, Reyna-Hurtado et al. 2017). They are differentiated from other extant African suids, among various craniodental and mandibular traits, in having bunolophodont and relatively hypsodont molars (Harris and White 1979; Thenius 1981; Souron 2012). Hypsodonty is a relative measure of tooth crown height and while *Hylochoerus* molars are

CONTACT Ignacio A. Lazagabaster Ignacio.Lazagabaster@mfn.berlin Museum Für Naturkunde, Leibniz Institute for Research on Evolution and Biodiversity, Invalidenstrasse 43, Berlin 10115, Germany

Supplemental data for this article can be accessed here.

Published online 22 Apr 2021

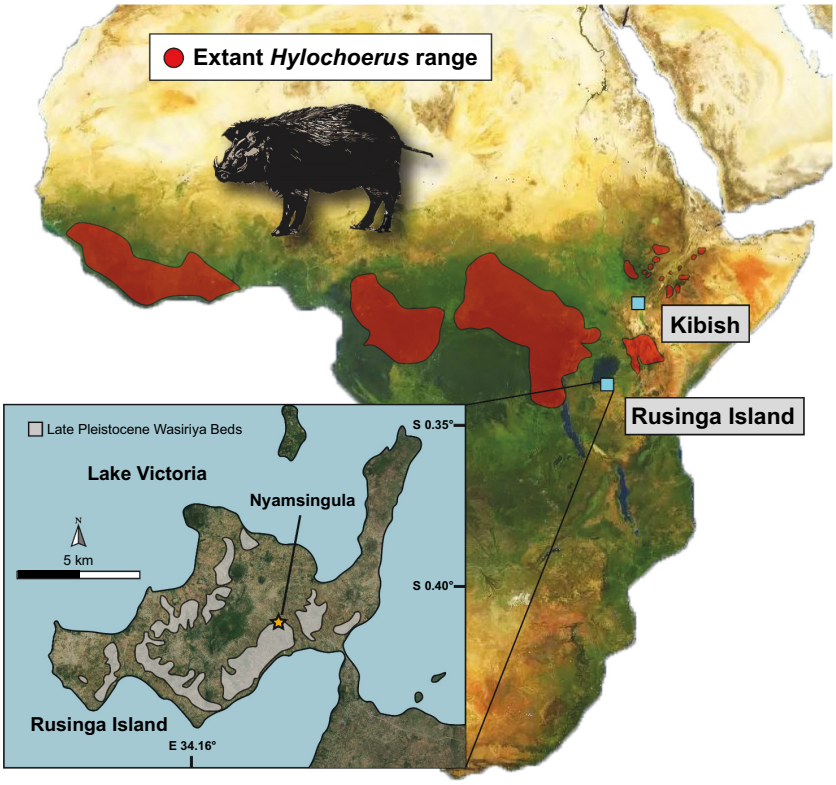

Figure 1. Map of Africa showing the current geographical distribution of extant *Hylochoerus* according to the IUCN and the location of fossil sites discussed, including Kibish, in Ethiopia, and the Late Pleistocene Wasiriya Beds and the Nyamsingula locality of Rusinga Island, in Kenya.

usually described as high-crowned, meticulous quantitative data on hypsodonty is lacking.

Hylochoerus likely descends from a lineage of bunolophodont suids formed by *Kolpochoerus phillipi* and its descendant *K. majus* that goes back at least 2.8 Ma. This lineage shows gradual evolution towards the mesiodistal compression of the molar main pillars, the elaboration of talon/id complexity, and the increase in coronal cementum cover thickness (Souron et al. 2015b; Lazagabaster et al. 2018). If the origin of *Hylochoerus* is traceable back to a *K. majus*-like ancestor, the characteristic features in the skull and the dentition of *Hylochoerus* must have evolved relatively rapidly during the Late Pleistocene. Unfortunately, the fossil record of *Hylochoerus* is very sparse. The only securely dated and well-identified fossils of *Hylochoerus* are those from Member III of the Kibish Formation ~0.1 Ma (Figure 1, Assefa et al. 2008). Therefore, the past diversity of *Hylochoerus* and the evolution of its derived craniomandibular and dental traits remain uncharted.

Here, we describe a distal fragment of a lower right third molar from Late Pleistocene (~50 to 36 ka) deposits at Rusinga Island, Kenya (Figure 1), that we attribute to an extinct form of *Hylochoerus*. We report for the first time rigorous *Hylochoerus* lower third molar hypsodonty values obtained from micro-CT scans and provide previously unpublished stable carbon isotopic data. These data allow us to discuss the importance of the fossil suid tooth in the context of the paleoenvironments at Rusinga and our understanding of the Late Pleistocene suid fossil record.

Depositional setting

The specimen was recovered in 2007 from the Late Pleistocene Wasiriya Beds at the Nyamsingula locality on Rusinga Island (Figure 1). Outcrops of the Wasiriya Beds are discontinuously exposed around the perimeter of Rusinga Island, typically ~15-36 m above the present-day level of Lake Victoria (Tryon et al. 2010, 2012). They document a succession of valley-fill sediments and tephra deposits, with the main lithologies including (1) poorly-sorted sandstones and conglomerates that represent phases of high-energy erosion and deposition in seasonal channels, (2) fine-grained sandstones and siltstones that have been pedogenically modified (i.e., poorly developed paleosols) and represent intervals of landscape stability, and (3) primary and variably reworked fine-grained tephra deposits that derive from sources in the Rift Valley (Tryon et al. 2010, 2012; Blegen et al. 2015). The maximum age of the Wasiriya Beds is constrained by U-series ages of 111–94 ka from a tufa deposit at the base of the sequence (Beverly et al. 2015), consistent with the composition of the basal Wakondo Tuff, which probably derives from eruptions of Mt. Suswa dated to 100 ± 10 ka (Blegen et al. 2015). The minimum age is provided by Menengai Tuff, which is at the top of the Wasiriya Beds sequence and has been $^{40}Ar/^{39}Ar$ dated to 35.62 ± 0.26 ka (Blegen et al. 2016). The

Table 1. Lower third molar summary metrics of selected extant and fossil Suidae.

	Length					Width					Height	Ref.
	n	min	max	mean	sd	n	min	max	mean	sd		
Fossil *Hylochoerus*												
Rusinga	1			>38					16.1		>29.2	a
Extant *Hylochoerus* (measured from micro-CT scans)												
Royal Museum for Central Africa	10	35	48	40.8	3.6	10	12	17	14.7	1.3	30	b
Museum für Naturkunde	4	36.8	43.3	41.1	2.5	4	14.4	15.7	14.9	0.5	29.6	a
Total	14	35	48	40.9	3.0	14	12	17	14.8	0.9	30	
Extant *Hylochoerus* (tooth inside the mandible, measured with caliper)												
Museum für Naturkunde	4	37.1	46.5	41.6	3.6	4	16	18.5	16.7	1.0		a
Field Museum of Natural History	4	42.1	51.2	46.8	3.1	4	17.9	18.5	18.3	0.2		a
Total	8	37.1	51.2	44.2	3.3	8	16	18.5	17.5	0.6		
Kolpochoerus majus												
Olduvai Bed I upper	1			42.5		1			20.7			c
Olduvai Bed II lower	1			43.5		1			20.3			c
Olduvai Bed II upper	3	45	50	48.3	2.9	3	21.7	22	21.8	0.1		c
Olduvai Bed III/IV	1			43		1			19.7			c
Daka	9	37.5	55.3	46.5	6.2	16	20.6	28.1	23.2	2	32.6	d
Buia	3	38.7	42.7	40.5	1.7	3	20.9	21.7	21.2	0.4	18	e
Total	18	37.5	55.3	44	3.6	25	20.6	28.1	21.15	0.8	32.6	
Kolpochoerus paiceae (=*K. olduvaiensis*)												
Omo-Shungura H	1			70		1			24.7			c
Omo-Shungura J	2	62.9	70.3	66.6	3.7	1			21			c
Omo-Shungura K	1			74		1						c
Omo-Shungura L	3	72.5	83.7	77.1	4.69	3	20.5	27.5	23.8	2.9		c
Koobi Fora Okote	4	67	72.6	69.6	2.2	4	22.4	25.3	24.1	1.1	35	f
Daka	10	50.9	82.4	67.8	11.8	17	18.3	28.6	23.1	3.3	37.7	d
Konso	5	61	65	62.6	1.3	4	22.5	23.5	22.9	0.4	27	g
Buia	7	50.9	66.8	58.8	5.8	7	10	17.7	14.8	2.7	17.7	e
Elandsfontein	15	63	77	71.6	4.7	15	21	25	22.9	1.2	36	h
Vaal River Gravels	2	68	70	69	1	2	21	22	21.5	0.5	35	h
Skurwerug	1	60	60	60		2	19	20	19.5	0.5		h
Total	52	50.9	83.7	67.9	3.9	57	10	28.6	21.8	1.6	37.7	

a, this publication; b, this publication. Data provided by A. Souron; c, Cooke (2007); d, Gilbert (2008); e, Medin et al. (2015); f, Harris (1983); g, Suwa et al. (2014); h, Hendey and Cooke (1985)

Table 2. Individual lower third molar measurements of extant *Hylochoerus* from CT-scans. Abbreviations: BL1 and BL2, buccolingual width of first and second lophid, respectively; H1 and H2, lingual height of first and second lophid, respectively; HI1 and HI2, hypsodonty index of first and second lophid, respectively. All measurements in mm.

Specimen	MD	BL1	BL2	H1	H2	HI1	HI2	Sex	Tooth side
MRAC 603	36	14	14	14	13	1.0	0.9		
MRAC 2226	43	16	16	24	23	1.5	1.4		
MRAC 2228	43	15	14	9	9	0.6	0.6		
MRAC 2490	40	15	15	14	14	0.9	0.9		
MRAC 2908	42	15	15	30	30	2.0	2.0		
MRAC 3418	38	14	14	13	13	0.9	0.9		
MRAC 13842	40	12	13	19	19	1.6	1.5		
MRAC 14002	48	17	16	30	30	1.8	1.9		
MRAC 15292	35	14	14	14	14	1.0	1.0		
MRAC 17783	43	15	16	21	20	1.4	1.3		
ZMB 39651	42.6	15.7	15.8	23.5	22.5	1.5	1.4	Male	R
ZMB 39653	36.8	14.7	14.6	28.9	27.9	2.0	1.9	Female	R
ZMB 83342	43.3	14.4	14.3	26.4	23.7	1.8	1.7	Female	R
ZMB 83343	41.7	14.8	14.9	29.6	27.2	2.0	1.8	Juvenile	R

sediments exposed at the Nyamsingula locality are stratigraphically above the ~50 ka Nyamita Tuff (Blegen et al. 2015, 2017) and suggest that the vertebrate fossils from this locality are between ~50 ka and ~36 ka in age.

Material and methods

Comparative specimens

We examined *Hylochoerus* mandibles from the mammal collections at the National Museum of Kenya, in Nairobi (n = 1), the Museum für Naturkunde in Berlin, Germany (n = 5), and the Chicago Field Museum, U.S.A. (n = 4). Additional fossil suid metrics were compiled from the literature (see references in Table 1). Third molar mesiodistal lengths were taken as maximal occlusal lengths, buccolingual widths were taken basally on the first and on the second pair of main lateral pillars, and heights were taken as maximal crown heights. All measurements were taken by one of us (I.A.L.) with digital calipers to ensure consistency. A summary of the metric data is given in Table 1.

Micro-computed tomography

Four *Hylochoerus* skulls were scanned using the YXLON FF35 CT computed tomography system in the Micro-CT Laboratory of the Museum für Naturkunde in Berlin, Germany. All scans have a resolution between 106 µm and 113 µm. Three specimens are adults (two females and one male) and the other is a juvenile (with the lower third molar still unerupted). Lower third molar morphology was examined by segmenting the tooth enamel using the grey value variation tool in VGStudio Max 3.3. Third molar mesiodistal lengths and buccolingual widths were taken close to the cervix. The height was measured from the middle point of the cusp at the cervix level to the top (occlusal part) of the cusp on the first and on the second pair of main lateral pillars (Figure 2). Additional metrics obtained in a similar fashion on *Hylochoerus* CT scans from the Royal Museum of Central Africa (n = 10) were kindly provided by A. Souron. The results are provided in Table 2 and summarised in Table 1.

Carbon and oxygen stable isotope analyses

Enamel from modern *Hylochoerus* (n = 12) and from the fossil specimen were analysed for $^{13}C/^{12}C$ and $^{18}O/^{16}O$ ratios using the conventional $\delta^{13}C$ and $\delta^{18}O$ notation where $\delta^{13}C = (R_{sample}/R_{standard} - 1) * 1000$ and R_{sample} and $R_{standard}$ are the $^{13}C/^{12}C$ ratios for the sample and the standard, respectively, with an analogous equation for $\delta^{18}O$, using the international reference material VPDB (Vienna Pee Dee Belemnite) as reference material. All samples were treated using conventional methods (Passey et al. 2002) in an area of about 5 mm x 1 mm x 0.5 mm (deep) mid-way from the cervix to the occlusal surface of the teeth. About 200 micrograms for each specimen were analysed using a Gas Bench at 50°C coupled to an Isotope Ratio Mass Spectrometer (IRMS). Temperature corrections for fossil and modern samples were made according to (Passey et al. 2007). The stable isotope results can be found in Appendix 1. In addition, a dataset of $\delta^{13}C$ and $\delta^{18}O$ values were compiled from the literature for extant and Pleistocene fossil African suid taxa, which includes the genera *Hylochoerus, Kolpochoerus, Phacochoerus, Potamochoerus*, and *Metridiochoerus* (Appendix 2). Note that taxonomic identifications have been updated by IAL and A. Souron and may differ from the original source. All $\delta^{13}C$ values for modern taxa are corrected to the pre-industrial $\delta^{13}C$ of atmospheric CO2 ($\delta^{13}C_{1,750}$).

Systematic palaeontology

Institutional Abbreviations – **FMNH**, Chicago Field Museum of Natural History, Chicago, USA. **KNM**, National Museums of Kenya, Nairobi, Kenya; **MRCA**, Royal Museum for Central Africa, Belgium; **ZMB**, Museum für Naturkunde, Berlin, Germany.

Dental terminology – Generally adapted from Harris and White (1979) and Boisserie et al. (2014).

Dental abbreviations – C, canines. I, incisors. P, premolars; M, molars; m3, lower third molar.

Class Mammalia Linnaeus 1758
Order Artiodactyla Owen 1848
Family Suidae Gray 1821
Genus *Hylochoerus* Thomas 1904

Generic diagnosis

Adapted from Souron (2012). Relatively large suid, especially among the Suinae, with marked sexual dimorphism; males can weigh over 250 kg. Cranio-mandibular structure derived with respect to *Potamochoerus* and *Sus*. Dental formula is reduced: 1/3I 1/1 C 3–2/2P 3/3 M. Incisors and mesial premolars reduced relative to *Potamochoerus*. Incisors less hypsodont than in *Potamochoerus*

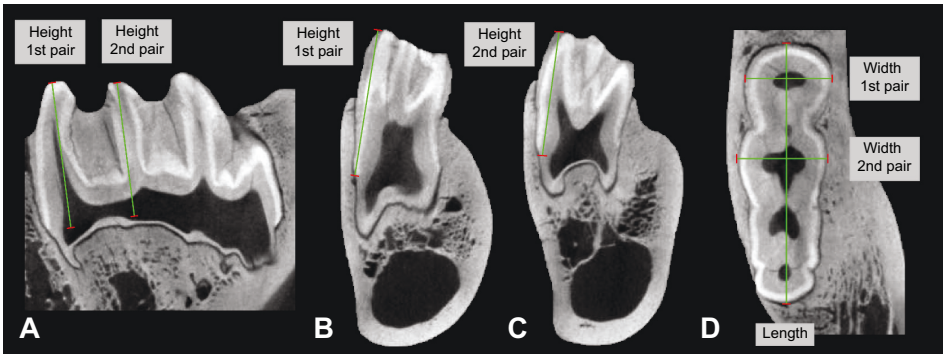

Figure 2. Lower third molar measurements taken on CT scans of extant *Hylochoerus*. The specimen pictured is the right lower third molar of ZMB 83342 in A) sagittal, B-C) coronal, and D) transverse planes.

or *Sus*, and with less lingual relief. Third molars elongated (longer than in *Potamochoerus*) and more hypsodont than *Potamochoerus*, but less than in *Phacochoerus*. Simple dental wear pattern, with mesiodistally compressed crown pillars and bunolophodont aspect. Developed troughs between main cusp rows, which are filled with coronal cement. Skull broad and short. Cross-section of the rostrum is rounded. Muscles of the rhinarium are reduced, leaving no marked insertions on the bones of the skull. Ridge of the supracanine process of males is reduced with respect to *Potamochoerus* and restricted to a low crest. Upper canine oriented laterally and somewhat dorsally. Zygomatic arch oriented slightly more obliquely to the sagittal plane of the skull than in *Potamochoerus*. In males, the zygomatic arch has significant mid-lateral expansions covered by rugose bone. Parietal wide between the temporal lines, and usually concave. Occipital relatively low and wide. Mandible with a relatively wide mandibular symphysis.

Hylochoerus sp.

Referred material

KNM-RU 49738, partial right lower third molar with collection number RU 2007-449 from Rusinga Island, Kenya, and curated at the National Museums of Kenya in Nairobi (Figure 3).

Locality and horizon

Late Pleistocene Wasiriya Beds at the Nyamsingula locality on Rusinga Island and dated to between ~50 ka and 36 ka (Figure 1).

Taxonomic remarks

The eastern African suid *K. limnetes* likely gave rise to two highly derived forms during the Pleistocene, the eastern African species *K. olduvaiensis* and its southern African counterpart *K. paiceae*. It has been suggested that there are no clear diagnostic characters separating these two species and that *K. olduvaiensis* is a junior synonym of *K. paiceae* (Souron 2012, 2017). We follow this recommendation here for simplicity, as it does not impact our anatomical comparative analyses.

Description

Specimen KNM-RU 49738 is a distal fragment of a right m3. There is marked space between pillar rows and the main pillars are mesiodistally compressed. The mesiodistal compression is stronger than the typical condition seen in the third molars of other derived kolpochoeres, including *K. majus* and *K. paiceae*, and resembles more the derived lophodonty of extant *Hylochoerus*. The occlusal morphology also matches that of extant *Hylochoerus* where the third molar main lateral pillars have mesial and distal invaginations of the enamel rim, though generally, suid tooth cusps (-ids) tend to have a simpler, rounded morphology as wear progresses. Nevertheless, in *K. majus* the third molar cusps (-ids) are more circular despite the mesiodistal compression. In *K. paiceae*, the cusp (-id) occlusal invaginations tend to get less marked towards the distal end of the third molar and the distal cusps (-ids) often show a certain degree of mesiodistal compression. In lateral view, the arrangement of pillars is somewhat reminiscent of other hypsodont suids, including *K. majus, K. paiceae, Metridiochoerus* spp., and *Phacochoerus* spp. The distal tapering of the tooth is like in *Hylochoerus* or *Kolpochoerus*, and unlike *Phacochoerus*. There is considerable coronal cementum cover occlusally, forming denser patches around and between cusps. Laterally, the coronal cementum cover is appreciably thinner and in some areas it is not preserved, revealing the corrugated enamel surface that is typical of other suids with cementum cover. In recent *Hylochoerus* there are usually cementum gaps between lateral cusps, though in some individuals, especially those with heavily worn teeth, the coronal cementum cover is extremely extended.

It is not possible to determine with certainty how much of the mesial part of the tooth is missing, whether it is missing one pair of main lateral pillars or more. The morphology of the apical portion of the tooth, however, provides a clue about this issue. In suines, the m3 cervix tends to be wider mesially, specifically close to the first and second pair of lateral pillars. Two examples showing extant *Hylochoerus* and *Sus scrofa* m3 axial sections at approximately the level of the cervix are pictured in Figure 3B-5 and 3C; the mesial widening is marked with a curved, dashed line. This widening reflects not only the larger size of the main four mesial cusps but also the larger size of the roots that support them. Distally to the first two pairs of laterals, the cervix outline continues more or less straight or narrows gradually towards the distal end of the tooth. This pattern mirrors what is seen in KNM-RU 49738 in apical view (Fig. 3A-6). Based on this comparison, we argue that the Rusinga m3 is likely missing just the first pair of lateral pillars (the metaconid and protoconid). We have restored an approximation of the occlusal outline of the mesial portion of the tooth using extant *Hylochoerus* m3s as template (Figure 3-A4 and 3-A5). The nomenclature used in the rest of the description below is followed based on this tentative reconstruction. We note that any conclusions derived from estimations of the length, the total number of main lateral pillars, or the morphology of the missing mesial portion of the tooth should be taken with caution.

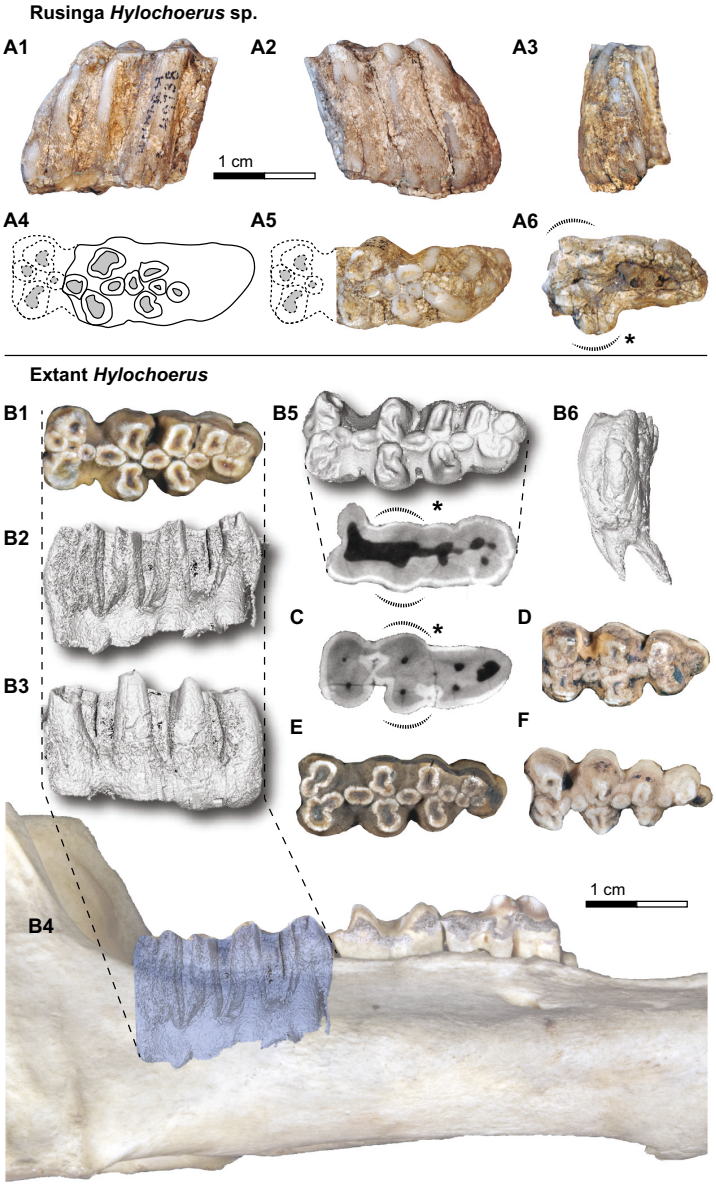

Figure 3. The right lower third molar fragment KNM-RU 49738 from Rusinga Island (A) and comparative lower third molars of extant *Hylochoerus* (B and D-F) and *Sus scrofa* (C). The fossil tooth in A1) buccal, A2) lingual, A3) distal, and A6) apical views, and A4-5) reconstruction of the missing mesial portion in occlusal views. Occlusal views of B1) ZMB 39651, D) ZMB 83342, E) ZMB 39652, and F) ZMB 39653. Right hemimandible of ZMB 39651 in lateral view (B4), with the lower third molar enamel extracted from micro-CT scans in B2) buccal, B3) lingual, B5) occlusal, and B6) distal views. Coronal cross-section at the level of the cervix in B7) ZMB 39651 and C) *Sus scrofa*.

We infer that the Rusinga m3 was composed of a total of four rows of main lateral pillars, which is typical in *Hylochoerus* and *K. majus*, while in *K. paiceae* there is at least an additional pair and usually two more pairs distally. There is, however, variation in this character in all the species mentioned. Examples of extant *Hylochoerus* m3s with only three and four pairs of main lateral pillars are shown in Figure 3(d-e). Distal to the presumed hypoconid and entoconid (the second pair of main lateral pillars), there is another pair of well-developed lateral pillars, though these are smaller and have a simpler morphology than their mesial counterparts. The tooth is terminated by three additional pillars. The one situated on the lingual side is larger and taller than the other two and the tip is already in occlusion. The buccal pillar is unworn but through wear progression, the lingual and buccal pillars would have formed another pair of main laterals. The distalmost pillar is shorter but has a wide base. There would have been two rounded median pillars (only the distal one and the distal portion of the mesial one are preserved) between the presumed first and second pair of main

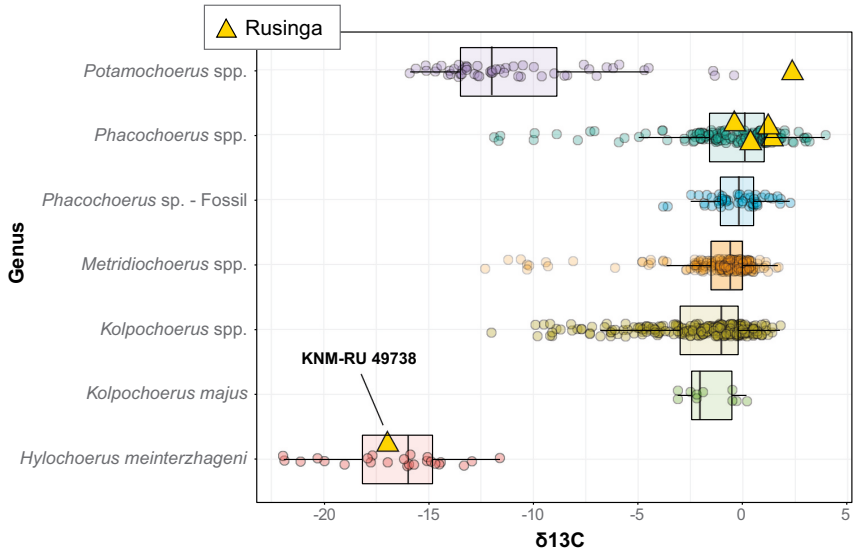

Figure 4. Stable carbon isotope values of Late Pleistocene Rusinga Island suids and comparative modern and fossil data for other African suid species and genera. The values shown for *Kolpochoerus* spp. do not include those of *K. majus*.

lateral pillars. This feature is present in *Hylochoerus* but also in other kolpochoeres, including *K. majus* and *K. paiceae*. Between the second and third pair of main lateral pillars, there is another pair of oval-shaped median pillars. The presence of one or two median pillars between rows of lateral pillars in the talonid is variable but occurs often in *K. majus, K. paiceae*, and other *Kolpochoerus*. In extant *Hylochoerus* there is generally only one single median pillar separating the second and third pair of laterals, but sometimes there can be two. One example is the *Hylochoerus* m3 pictured in Souron et al. (2015a: Figure 1(c)).

The mesiodistal length of the preserved fragment is 38 mm. The total length cannot be accurately estimated but, in our reconstruction, the tooth would have been between 46–50 mm long. This is in the upper range of extant *Hylochoerus* and *K. majus* m3 metrics. The m3 mesiodistal length average of extant *Hylochoerus* in our dataset is 40.9 ± 3.0 mm (n = 14), with a specimen reaching 48 mm (Table 1). The m3 mesiodistal length average is 40.9 ± 3.0 mm (n = 14) in *Hylochoerus*, 44.0 ± 3.6 mm in *K. majus* (n = 18), and 67.9 ± 3.9 mm in *K. paiceae* (n = 52), with individual specimens reaching 48.0 mm, 55.3 mm, and 83.7 mm, respectively. It is noteworthy that our extant *Hylochoerus* m3 metrics derive from basal measurements taken on CT-scans, while most published measurements were taken with calipers and occasionally on specimens that had the base still inside the mandible and not visible. The different approaches can produce results that are not directly comparable. To demonstrate this point, we remeasured the m3s of the four scanned *Hylochoerus* individuals with a caliper on the original specimens. We show that there can be a significant overestimation of the m3 length (max m3 length: 43.3 mm from CT-scans, 46.5 mm with a caliper) and width (15.7 mm from CT-scans, 18.5 mm with a caliper).

The hypsodonty index (HI) is calculated through the division of the maximum unworn crown height by its buccolingual width at the base. The maximum crown height in KNM-RU 49738 is 26.3 mm labially and 29.2 mm lingually. However, the tooth is slightly to moderately worn and the estimated maximum height without wear would have been between 30 to 32 mm. The buccolingual width at the base is normally measured on the anterior portion of the tooth, which in the case of KNM-ER 49738 is missing. For this reason, we use the width at the base of the presumed second pair of main lateral pillars (in our reconstruction), which measures 16.1 mm. In a sample of *H. meinertzhageni* (n = 8), the difference between the width of the first and second lophid is negligible (Table 2; 17.5 mm and 17.9 mm respectively). The resultant HI of the fossil specimen is between 1.8 to 2.0. This HI estimation is considerably higher than the HI value of 1.36 for *H. meinertzhageni* reported in Janis (1988), with a maximum m3 height of 21 mm. The m3s examined in Janis (1988) must have had a certain amount of wear and/or were still inside the mandible, evidently producing underestimations of height and overestimations of width. The data derived from CT-scans presented here, however, indicate that extant *Hylochoerus* teeth are as high as 30 mm (Table 2), with a HI up to 2.0. The derived kolpochoeres *K. majus* and *K. paiceae* m3s can also reach this height, though in *K. majus* it is a rare condition while in *K. paiceae* m3 crowns are often taller. The hypsodonty of the Rusinga tooth is therefore compatible with extant *Hylochoerus* but also with other derived Pleistocene kolpochoeres.

Taxonomic discussion

According to Souron et al. (2015b), the origin of *Hylochoerus* dates to the Late Pliocene *K. afarensis*, which gave rise to a lineage of bunolophodont suids composed of two chronospecies, *K. phillipi* and *K. majus*. The species *K. phillipi* is known from the Ethiopian sites of Ledi Geraru ~2.8–2.6 Ma (Lazagabaster et al. 2018) and Matabaietu ~2.5 Ma (Souron et al. 2015b). The dental morphology of the Konso material ~1.9 Ma is morphologically intermediate between *K. phillipi* and *K. majus* (Suwa et al. 2014), while more typical *K. majus* is found throughout various eastern African sites dating from 1.8 Ma to *ca*. 0.5 Ma: Olduvai Beds I–IV, in Tanzania (Leakey 1942; Cooke 2007; Bibi et al. 2018); the Upper Lomekwi and Nariokotome Mbs. in West Turkana and Olorgesailie, in Kenya

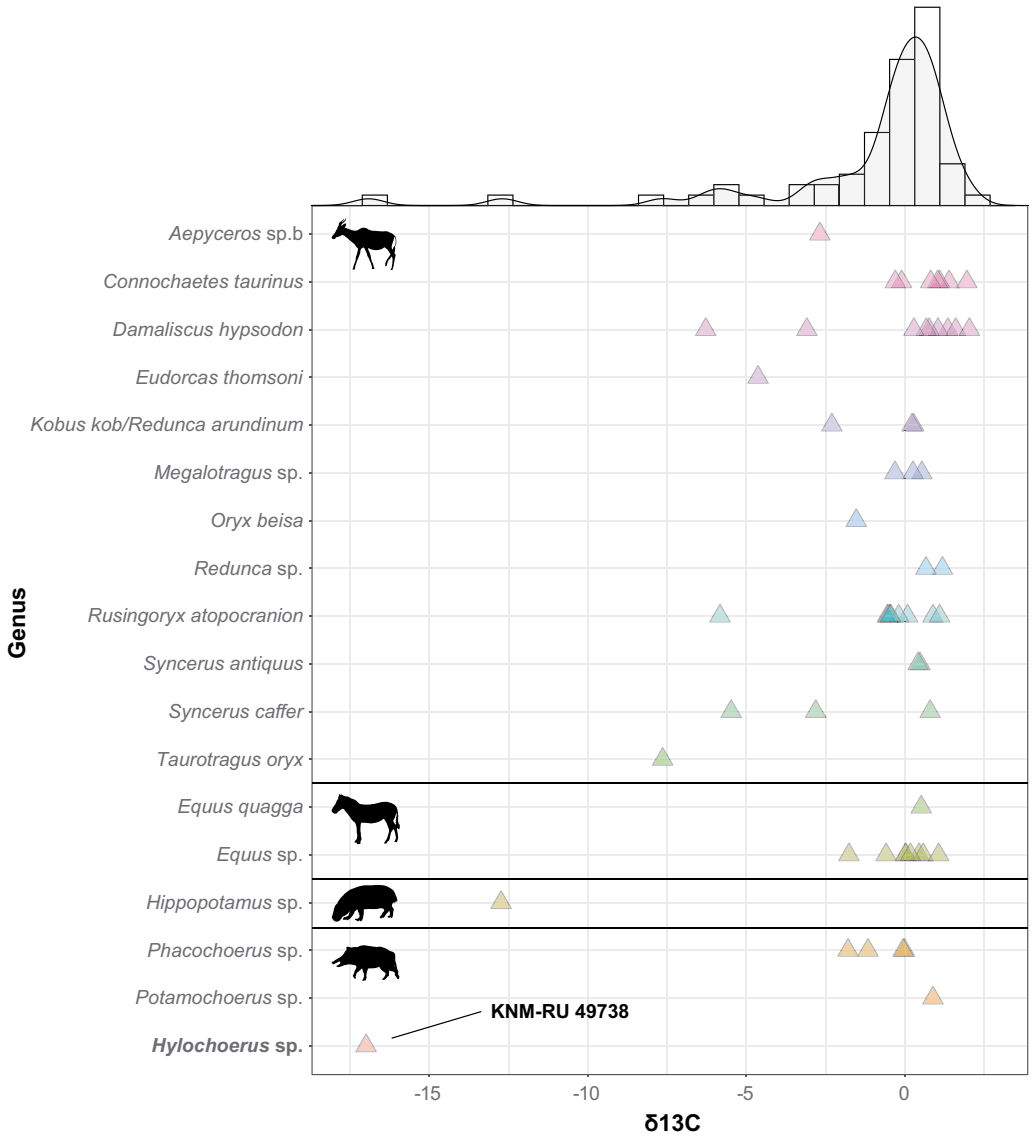

Figure 5. Stable carbon isotope values of Late Pleistocene Rusinga Island large mammals, including Bovidae, Equidae, Hippopotamidae, and Suidae.

(Harris and White 1979; Harris et al. 1988; Souron 2012; Potts et al. 2018); Buia, in Eritrea (Medin et al. 2015); Mb. L of the Shungura Fm., the Busidima Fm. at Gona and Asbole, the Lower Herto and Daka Mbs. and the upper Bodo beds of the Bouri Fm., in the Middle Awash, and the Melka-Kunture Fm. of Garba IV, in Ethiopia (Harris and White 1979; Clark et al. 1994; White 1995; Geraads et al. 2004a, 2004b; Gilbert 2008; Everett 2010; Souron 2012). Some undescribed specimens from the Middle Awash ~0.1 Ma in Ethiopia may also be attributed to *K. majus* (Souron et al. 2015b). Sometime possibly during the Middle to Late Pleistocene, a population of *K. majus* likely gave rise to *Hylochoerus* but the only securely identified fossil remains of *Hylochoerus* are those from Kibish, in Ethiopia, also dated to ~0.1 Ma (Assefa et al. 2008).

The m3 from Rusinga described here was briefly noted in Faith's (2014) overview of extinct Late Pleistocene African mammals. He reported it as *Kolpochoerus*, suggesting that the level of compression of the pillars and cementum most closely resembled *K. majus*. However, our reanalysis indicates that the mesiodistal compression of the main pillars and the distance between pillar rows are more accentuated than in *K. majus* third molars, and the occlusal morphology – with mesiodistal invaginations – aligns this tooth better with *Hylochoerus*. In *K. paiceae*, the m3 distal cusps can sometimes show mesiodistal compression but not to the degree of the Rusinga tooth. Furthermore, *K. paiceae* teeth tend to be longer and more hypsodont than our estimated metrics. Other Plio-Pleistocene suid genera, *Metridiochoerus* spp., and *Phacochoerus* spp., have taller crowns than KNM-RU 49738 and the main lateral pillars are not mesiodistally compressed. Unfortunately, the fragmentary nature of this fossil does not allow us to compare absolute numbers with confidence. For this reason, further specific taxonomic attribution of the Rusinga specimen is not feasible, especially considering that the taxonomic configuration of extant forest hogs has not been fully resolved (Reyna-Hurtado et al.

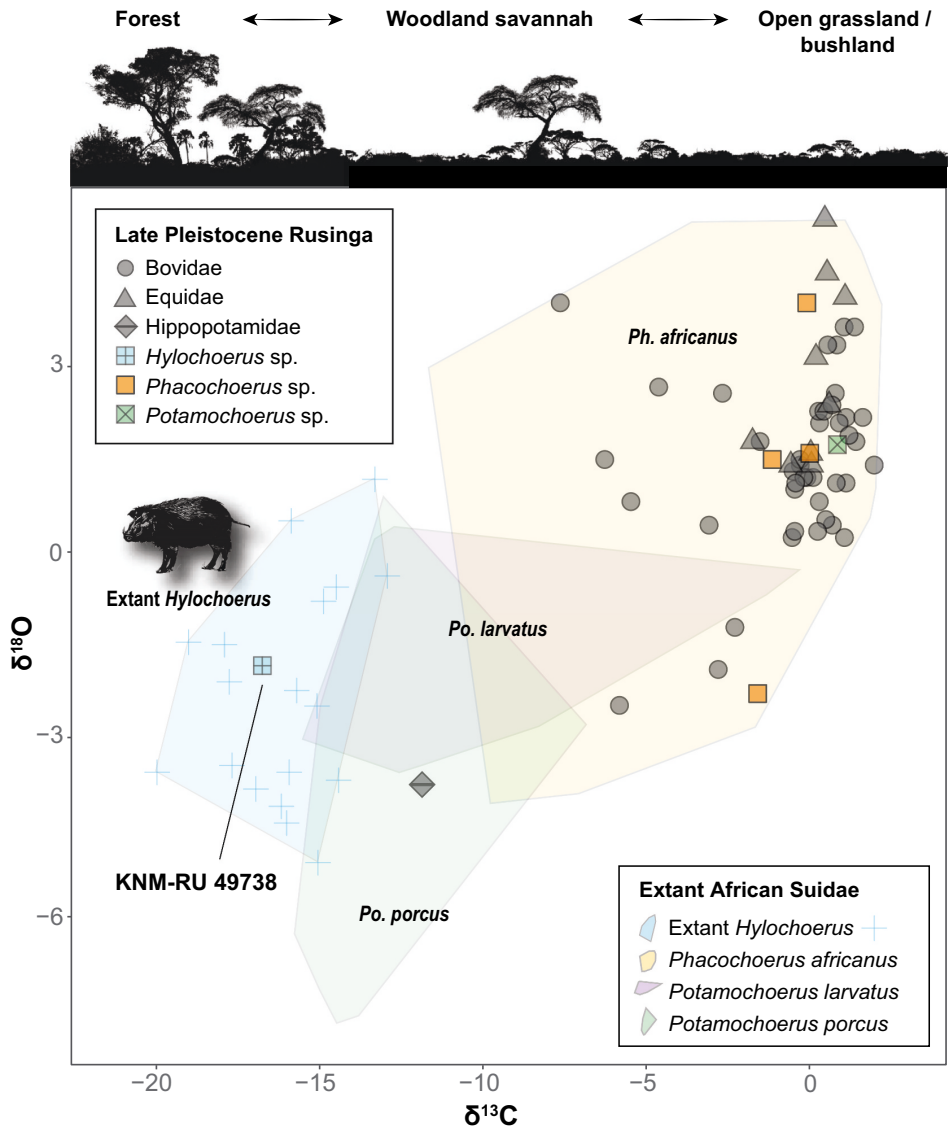

Figure 6. Stable carbon and oxygen isotope values of Late Pleistocene Rusinga Island large mammals and extant African Suidae. Note that KNM-RU 49738 falls within the range of variation of extant *Hylochoerus*.

2017). Distal third molar fragments can sometimes share similar morphologies across different suid genera. Given the great intra-specific variability in extant and fossil suid third molars (Harris and White 1979), the possibility that this tooth belongs to another late-surviving *Kolpochoerus* lineage (e.g., *K. paiceae*) should be taken into consideration, though we find this hypothesis unlikely. *Kolpochoerus paiceae* evolved elongated third molars with tall-columnar pillars and cementum cover that resemble those of *Metridiochoerus* spp. (Souron 2012), which have resulted in several misidentifications (e.g., in Omo-Shungura suids, Cooke 2007). The latest known *K. paiceae* remains, however, are dated to 0.8 Ma (Souron 2012).

Palaeoecology and paleoenvironment: stable isotope analyses

Plants that use the C_3 photosynthetic pathway (tropical dicots: trees, bushes, herbs) differ in their discrimination against $^{13}CO_2$ from plants that use the C_4 photosynthetic pathway (tropical grasses and sedges). C_4 photosynthesis is typically prevalent in warm and seasonally dry, open habitats, whereas C3-plants dominate in conditions of lower water stress, cooler ground temperatures, and closed canopy (Pearcy and Ehleringer 1984; Cerling et al. 2011; Uno et al. 2011). In large mammals, higher enamel $\delta^{13}C$ are

associated with C_4-plant eaters (e.g., grazers; generally $\delta^{13}C > -1$ ‰) while more negative $\delta^{13}C$ values are found in the enamel of C_3-plant consumers (e.g., browsers; generally $\delta^{13}C < -8$ ‰; Cerling et al. 2015).

The $\delta^{13}C$ of KNM-RU 49738 is −17.0 ‰, which is well within the range of extant *Hylochoerus*, with an average of −16.7 ± 2.5 ‰ for 24 modern specimens corrected to the pre-industrial value and a range between −13.6 ‰ and −22.6 ‰ (Figure 4). The extremely negative $\delta^{13}C$ value for KNM-RU 49738 contrasts with most of the other large herbivores at Rusinga Island, with an average $\delta^{13}C$ value of −0.7 ± 2.6 ‰ (n = 58; Figure 5; data from Garrett et al. 2015). This is one of the most negative $\delta^{13}C$ values for any fossil tooth enamel from Africa; other herbivores with such negative values are found in cave deposits in Southeastern Asia and are interpreted as being associated with closed canopy conditions (Bocherens et al. 2017; Ma et al. 2017, 2019; Bacon et al. 2018). Thus, this particular sample presents an interesting puzzle for interpretation since there is no other clear evidence for closed-canopy conditions in the associated fauna or isotopes, and most lines of evidence point to relatively dry conditions and an expansion of C_4 grasslands across the Lake Victoria basin during the Late Pleistocene (e.g., Tryon et al. 2010, 2012, 2016; Faith et al. 2015, 2020; Garrett et al. 2015; Beverly et al. 2017). The Rusinga *Hylochoerus* may derive from sediments reflecting a humid phase that is otherwise not represented by the faunas, but analysis of paleosols from Rusinga and nearby Karungu indicate that relatively dry conditions persisted from ~94-36 ka (Beverly et al. 2017). The complete absence of Later Stone Age artefacts (dating from < 36 ka in the region; Tryon et al. 2016; Blegen et al. 2017) at Nyamsingula also suggests that it is unlikely the specimen derives from undocumented or eroded Holocene deposits that sample a more humid climate with closed habitats.

Other alternative hypotheses that could result in comparable negative $\delta^{13}C$ signals are selective diets of C_3 plants in arid open environments or C_3 graminoids or forbs in open but humid environments (e.g., close to water bodies that provide shade and humidity; Souron 2018). The consumption of aquatic plants can also result in negative $\delta^{13}C$ values (Chappuis et al. 2017). In modern tropical lowland African ecosystems, C_3 herbaceous plants are generally scarce (abundance < 10%, Sage et al. 1999). However, C_3 graminoids, forbs, and ferns, can be relatively abundant in certain savannah ecosystems (e.g., Kruger National Park; Codron et al. 2005) and in some lowland African Plio-Pleistocene habitats (Bonnefille 2010; Feakins et al. 2013; Albert et al. 2015; Lüdecke et al. 2016; Magill et al. 2016). To our knowledge, however, there are no records of extant *Hylochoerus* feeding on aquatic plants or consistently venturing on open habitats to feed (D'Huart 1978; Kingdon 1979; D'Huart and Kingdon 2013; Reyna-Hurtado et al. 2017).

The Plio-Pleistocene suids with the most negative $\delta^{13}C$ are those from the Karonga basin in the Malawi Rift (Lüdecke et al. 2016), Elandsfontein in the southwestern Cape of South Africa (Luyt et al. 2000), and Aramis in the Middle Awash, Ethiopia (White et al. 2009). The case of Elandsfontein is unique because the southwestern Cape has long had a winter rainfall regime that favours C_3 grasses and dicots (Luyt et al. 2000; Lehmann et al. 2016); today the region is dominated fynbos, renosterveld, and strandveld plant communities that unlike anything found in eastern Africa. In the case of Karonga and Aramis, these negative $\delta^{13}C$ have been interpreted as reflecting closed-canopy habitats and gallery forests respectively (Luyt et al. 2000; White et al. 2009). Furthermore, forest/closed canopy species tend to have more negative $\delta^{13}C$ than open-habitat species. For example, duikers (*Cephalophus* spp.), which inhabit rainforests and forests, display more negative $\delta^{13}C$ than the eland (*Taurotragus oryx*), a woodland-savanna species (Cerling et al. 2003). Both bovids, however, are almost exclusive C_3 feeders. In Queen Elizabeth National Park in Uganda, which has both warthogs and forest hogs, where the forest hogs are living near the boundary of grassland/forest, the $\delta^{13}C$ values are enriched ($\delta^{13}C = -12$ to −13 ‰; Cerling and Viehl 2004). These results suggest that the fossil forest hog would have consumed C_4 resources if it had inhabited open grasslands. Therefore, the extremely negative $\delta^{13}C$ of KNM-RU 49738 is most likely an indication of the presence of closed canopy.

The $\delta^{18}O$ of KNM-RU 49738 is −1.9 ‰, which is also comparable to the values of extant *Hylochoerus*, with an average of −2.6 ± 1.8 ‰ (n = 22; Figure 6). Oxygen isotopes in palaeoecological contexts are generally associated with external water dependency (Sponheimer and Lee-Thorp 1999, 2001; Harris and Cerling 2002). Variations in oxygen isotope composition of mammalian tooth enamel are mainly a function of the oxygen isotope composition of food and liquid water. Leaf $\delta^{18}O$ water is enriched (typically 10–30% more) in comparison to the meteoric source (Epstein et al. 1977; Yakir and Others 1998). Thus, mammal species that obtain the majority of their water from the plants they eat should display more positive $\delta^{18}O$ in comparison to obligate drinkers (Sponheimer and Lee-Thorp 1999, 2001; Harris and Cerling 2002). In African bovids, browsers tend to show more enriched $\delta^{18}O$ than do grazers. Interestingly, in African suids the patterns seem to be reversed: taxa that inhabit forested habitats (*Hylochoerus, Po. porcus*, and some populations of *Po. larvatus*) have generally low values of both $\delta^{18}O$ and $\delta^{13}C$ (Figure 6), while both ratios get higher in grazer taxa (*Ph. africanus* and some populations of *Po. larvatus*). Nevertheless, KNM-RU 49738 fits clearly in the isotope ecospace of extant *Hylochoerus* (with negative $\delta^{18}O$ and $\delta^{13}C$). It is worth mentioning that the only hippopotamid sampled in Rusinga also has negative values of $\delta^{18}C$ and $\delta^{13}O$ that are close to those of *Hyochoerus* (Figures 5–6; Garrett et al. 2015). The values for this tooth are also extremely negative points among Plio-Pleistocene African hippopotamids (e.g., Harris et al. 2008; Cerling et al. 2008, 2015); such negative values are more common in C3-grazers in swampy habitats (e.g., the pigmy hippopotamus *Choeropsis liberiensis*). The presence of grassy/sedgy wetlands, therefore, cannot be completely ruled out.

The most likely explanation for the presence of *Hylochoerus* on Rusinga, and its very negative $\delta^{13}C$ value, is that the Late Pleistocene environment was more heterogeneous than previously considered. At the Nyamita locality (~3 km SW of Nyamsingula), spring-fed rivers and wetlands promoted locally dense vegetation cover of the sort that could favour *Hylochoerus*, including woody vegetation, as well as grasses and sedges (Beverly et al. 2015; Garrett et al. 2015). This alone may not explain the $\delta^{13}C$ value, so it is also plausible that there were some patches of closed-canopy forest in the highlands on Rusinga where Pleistocene deposits are not found.

Conclusions

Despite being a single and fragmented specimen, the lower third molar crown morphology of the Rusinga fossil – namely, its bunolophodont aspect – matches that of extant *Hylochoerus* third molars. We show that its crown height and hypsodonty index were as high as those of extant forest hogs. The acquired hypsodonty in the *K. phillipi-K.majus-Hylochoerus* lineage mirrors what happened in multiple African suid lineages since the Miocene (Harris and White 1979; Souron et al. 2015b; Souron 2017; Lazagabaster et al. 2018), though not to the extreme of some derived taxa (e.g., *Notochoerus scotti, Metridiochoerus compactus* or *Phacochoerus*). What is unique about *Hylochoerus* among African suids is its derived lophodonty. *Kolpochoerus* is usually associated with open-grassland to mixed savannah habitats after 2.5 Ma, and stable

carbon isotopes suggest its diet was mainly composed of C_4 resources (Harris and Cerling 2002; Bibi et al. 2013; Cerling et al. 2015; Lazagabaster 2019; Negash et al. 2020). While multiple suid taxa were evolving adaptations to eating more abrasive foods in the context of C_4-grasslands expansion in Africa, the available fossil evidence suggests that *Hylochoerus* turned away from the open habitats and into the forests. Comprehending exactly when and how did this happen is currently unattainable, as the third molar described here and the remains from Kibish are the only *Hylochoerus* fossil remains known to date (Assefa et al. 2008). The association of *Hylochoerus* with closed habitats (D'Huart 1993; Cerling and Viehl 2004; D'Huart and Kingdon 2013; D'Huart and Yohannes 2014; Frantz et al. 2016) may explain why its fossil record is so sparse and provide new insights into the paleoenvironmental at Rusinga, which appears to have been more heterogeneous than typically considered.

The Rusinga *Hylochoerus* adds to a growing body of evidence showing that geologically recent faunas are quite different from those of the present-day (Faith 2014; Faith et al. 2019, 2020). Extant species, including the Rusinga *Hylochoerus*, are often found well outside their historic ranges (e.g., Rowan et al. 2015; Lesur et al. 2016; Faith et al. 2020) – leading to the formation of non-analogue species combinations – and it is becoming increasingly clear that extinct species were numerous (Faith 2014). Considerable work remains ahead if we are to sort out the emergence of what we would recognise as 'modern' eastern African faunal communities and the impact of terminal Pleistocene climatic changes in the present configuration of African ecosystems.

Acknowledgments

IAL acknowledges a Humboldt Postdoctoral Fellowship. JTF acknowledges support from the Natural History Museum of Utah. The stable isotope work was supported by a National Science Foundation grant #1740383 and the research permit is NACOSTI//P18/95520/23873. We thank Kevin Uno and Julia Tejada for assistance in sampling. We thank the curatorial team a the National Museums of Kenya. We thank Kristin Mahlow from the Micro-CT Laboratory at the Museum für Naturkunde, and the mammal collections curatorial team, including Frieder Mayer, Doreen Breyer, and Detlef Willborn. We thank two anonymous reviewers and Antoine Souron for his critical comments and for sharing unpublished data obtained from CT-scans, which were obtained with the help of Emmanuel Gilissen and Wim Wendelen (MRAC, Tervuren), Franck Guy (PALEVOPRIM, Univ. Poitiers), and Walter Coudyzer (Universitair Ziekenhuis Leuven). We thank John Rowan and Valentina Rovelli for their suggestions and support. Lastly, we thank those who contributed to the collection of Pleistocene faunas from Rusinga Island, including Nick Blegen, Holly Dunsworth, Will Harcourt-Smith, Kirsten Jenkins, Tom Lehmann, Kieran McNulty, Dan Peppe, and Christian Tryon.

Data availability statement

All data used in this publication is reported in the text and in Appendices 1 and 2. Supplementary datasets (Appendix 1 and Appendix 2) are also available at a permanent repository: https://osf.io/rcjts/

Disclosure statement

The authors declare no competing interests.

Funding

This work was supported by the National Science Foundation [1740383]; Alexander von Humboldt-Stiftung.

ORCID

Ignacio A. Lazagabaster http://orcid.org/0000-0001-9149-7371
Thure E. Cerling http://orcid.org/0000-0002-3590-294X
J. Tyler Faith http://orcid.org/0000-0002-1101-7161

References

Albert RM, Bamford MK, Stanistreet I, Stollhofen H, Rivera-Rondón C, Rodríguez-Cintas A. 2015. Vegetation landscape at DK locality, Olduvai Gorge, Tanzania. Palaeogeogr Palaeoclimatol Palaeoecol. 426:34–45. doi:10.1016/j.palaeo.2015.02.022.

Assefa Z, Yirga S, Reed KE. 2008. The large-mammal fauna from the Kibish Formation. J Hum Evol. 55(3):501–512. doi:10.1016/j.jhevol.2008.05.015.

Bacon A-M, Bourgon N, Dufour E, Zanolli C, Duringer P, Ponche J-L, Antoine P-O, Shackelford L, Huong NTM, Sayavonkhamdy T, et al. 2018. Nam Lot (MIS 5) and Duoi U'Oi (MIS 4) southeast Asian sites revisited: zooarchaeological and isotopic evidences. Palaeogeogr Palaeoclimatol Palaeoecol. 512:132–144. doi:10.1016/j.palaeo.2018.03.034.

Beverly EJ, Driese SG, Peppe DJ, Arellano LN, Blegen N, Faith JT, Tryon CA. 2015. Reconstruction of a semi-arid late Pleistocene paleocatena from the Lake Victoria region, Kenya. Quat Res. 84:368–381. doi:10.1016/j.yqres.2015.08.002.

Beverly EJ, Peppe DJ, Driese SG, Blegen N, Faith JT, Tryon CA, Stinchcomb GE. 2017. Reconstruction of late pleistocene paleoenvironments using bulk geochemistry of paleosols from the Lake Victoria region. Front Earth Sci Chin. 5:93. doi:10.3389/feart.2017.00093.

Bibi F, Pante M, Souron A, Stewart K, Varela S, Werdelin L, Boisserie J-R, Fortelius M, Hlusko L, Njau J, et al. 2018. Paleoecology of the serengeti during the oldowan-acheulean transition at Olduvai Gorge, Tanzania: the mammal and fish evidence. J Hum Evol. 120:48–75. doi:10.1016/j.jhevol.2017.10.009.

Bibi F, Souron A, Bocherens H, Uno K, Boisserie J-R. 2013. Ecological change in the lower Omo Valley around 2.8 Ma. Biol Lett. 9:20120890. doi:10.1098/rsbl.2012.0890.

Bishop LC. 2010. Suoidea. In: Werdelin L, Sanders W, editors. Cenozoic mammals of Africa Univ of California press. Berkeley: University of California Press Berkeley; p. 829–850.

Blegen N, Brown FH, Jicha BR, Binetti KM, Faith JT, Ferraro JV, Gathogo PN, Richardson JL, Tryon CA. 2016. The Menengai Tuff: a 36 ka widespread tephra and its chronological relevance to Late Pleistocene human evolution in East Africa. Quat Sci Rev. 152:152–168. doi:10.1016/j.quascirev.2016.09.020.

Blegen N, Faith JT, Mant-Melville A, Peppe DJ, Tryon CA. 2017. The middle stone age after 50,000 years ago: new evidence from the Late Pleistocene sediments of the eastern Lake Victoria basin, Western Kenya. PaleoAnthropology. 139–169. doi:10.4207/PA.2017.ART108

Blegen N, Tryon CA, Faith JT, Peppe DJ, Beverly EJ, Li B, Jacobs Z. 2015. Distal tephras of the eastern Lake Victoria basin, equatorial East Africa: correlations, chronology and a context for early modern humans. Quat Sci Rev. 122:89–111. doi:10.1016/j.quascirev.2015.04.024.

Bocherens H, Schrenk F, Chaimanee Y, Kullmer O, Mörike D, Pushkina D, Jaeger J-J. 2017. Flexibility of diet and habitat in Pleistocene south Asian mammals: implications for the fate of the giant fossil ape Gigantopithecus. Quat Int. 434:148–155. doi:10.1016/j.quaint.2015.11.059.

Boisserie J-R, Souron A, Mackaye HT, Likius A, Vignaud P, Brunet M, Rook L. 2014. A new species of *Nyanzachoerus* (Cetartiodactyla: suidae) from the late Miocene Toros-Ménalla, Chad, central Africa. PLoS One. 9:e103221. doi:10.1371/journal.pone.0103221.

Bonnefille R. 2010. Cenozoic vegetation, climate changes and hominid evolution in tropical Africa. Glob Planet Change. 72:390–411. doi:10.1016/j.gloplacha.2010.01.015.

Butynski TM, Jong YAD. 2017. Warthog *Phacochoerus africanus*. In: Melletti M, Meijaard E, editors. Ecology, conservation and management of wild pigs and peccaries. Cambridge: Cambridge University Press; p. 85–100.

Cerling TE, Andanje SA, Blumenthal SA, Brown FH, Chritz KL, Harris JM, Hart JA, Kirera FM, Kaleme P, Leakey LN, Others. 2015. Dietary changes of large herbivores in the Turkana Basin, Kenya from 4 to 1 Ma. Proc Natl Acad Sci U S A. 112:11467–11472. doi:10.1073/pnas.1513075112.

Cerling TE, Harris JM, Hart JA, Kaleme P, Klingel H, Leakey MG, Levin NE, Lewison RL, Passey BH. 2008. Stable isotope ecology of the common hippopotamus. J Zool. 276:204–212. doi:10.1111/j.1469-7998.2008.00450.x.

Cerling TE, Harris JM, Passey BH. 2003. Diets of East African Bovidae based on stable isotope analysis. J Mammal. 84:456–470. doi:10.1644/1545-1542(2003)084<0456:DOEABB>2.0.CO;2.

Cerling TE, Viehl K. 2004. Seasonal diet changes of the forest hog (*Hylochoerus meinertzhageni* Thomas) based on the carbon isotopic composition of hair. Afr J Ecol. 42:88–92. doi:10.1111/j.1365-2028.2004.00500.x.

Cerling TE, Wynn JG, Andanje SA, Bird MI, Korir DK, Levin NE, Mace W, Macharia AN, Quade J, Remien CH. 2011. Woody cover and hominin environments in the past 6 million years. Nature. 476:51–56. doi:10.1038/nature10306.

Chappuis E, Seriñá V, Martí E, Ballesteros E, Gacia E. 2017. Decrypting stable-isotope ($\delta^{13}C$ and $\delta^{15}N$) variability in aquatic plants. Freshw Biol. 62:1807–1818.

Clark JD, Heinzelin JD, Schick KD, Hart WK, White TD, WoldeGabriel G, Rc W, Suwa G, Asfaw B, Vrba E. 1994. African *Homo erectus*: old radiometric ages and young Oldowan assemblages in the Middle Awash Valley, Ethiopia. Science. 264:1907–1910. doi:10.1126/science.8009220.

Codron J, Codron D, Lee-Thorp JA, Sponheimer M, Bond WJ, Ruiter DD, Grant R. 2005. Taxonomic, anatomical, and spatio-temporal variations in the stable carbon and nitrogen isotopic compositions of plants from an African savanna. J Archaeol Sci. 32:1757–1772. doi:10.1016/j.jas.2005.06.006.

Cooke HBS. 2007. Stratigraphic variation in Suidae from the Shungura Formation and some coeval deposits. In: Bobe R, Alemseged Z, Behrensmeyer AK, editors. Hominin Environments in the East African Pliocene: an Assessment of the Faunal Evidence. Dordrecht: Springer Netherlands; p. 107–127.

Cumming DHM. 1975. A field study of the ecology & behaviour of warthog. Salisbury: Trustees of the National Museums and Monuments of Rhodesia.

Cumming DHM.. 2013. *Phacochoerus africanus* common warthog. In: Kingdon J, Happold D, Butynski T, Hoffmann M, Happold M, Kalina J, editors. Mammals of Africa. Vol. 6. London: Bloomsbury Publishing; p. 54–60.

D'Huart JP. 1978. Ecologie de l'hylochère: *hylochoerus meinertzhageni* Thomas au Parc national des Virunga. Exploration PNV, Deuxième Série, Fasc. 25. Brussels: Fundation pour favoriser les recherches scientifiques en Afrique; p. 156.

D'Huart JP. 1993. The forest hog (*Hylochoerus meinertzhageni*). In: Oliver WLR, editor. Pigs, peccaries and hippos: status survey and conservation action plan. Gland (Switzerland): IUCN; p. 84–92.

D'Huart JP, Kingdon J. 2013. *Hylochoerus meinertzhageni* forest hog. In: Kingdon J, Happold D, Butynski T, Hoffmann M, Happold M, Kalina J, editors. Mammals of Africa. Vol. 6. London: Bloomsbury Publishing; p. 42–49.

D'Huart JP, Yohannes E. 2014. Assessment of the present distribution of the Forest hog (*Hylochoerus meinertzhageni*) in Ethiopia. J Mt Ecol. 3:46–48.

Epstein S, Thompson P, Yapp CJ. 1977. Oxygen and hydrogen isotopic ratios in plant cellulose. Science. 198:1209–1215. doi:10.1126/science.198.4323.1209.

Everett MA 2010. The paleoecology of the Pleistocene upper busidima formation, gona, afar depression, Ethiopia. PhD Thesis, Indiana University.

Ewer RF. 1958. Adaptive features in the skulls of African suidae. Proc Zool Soc Lond. 131:135–155. doi:10.1111/j.1096-3642.1958.tb00637.x.

Ewer RF. 1970. The head of the forest hog, *Hylochoerus meinertzhageni*. Afr J Ecol. 8:43–52. doi:10.1111/j.1365-2028.1970.tb00829.x.

Faith JT. 2014. Late Pleistocene and Holocene mammal extinctions on continental Africa. Earth-Sci Rev. 128:105–121.

Faith JT, Rowan J, Du A. 2019. Early hominins evolved within non-analog ecosystems. Proc Natl Acad Sci U S A. 116:21478–21483. doi:10.1073/pnas.1909284116.

Faith JT, Rowan J, O'Brien K, Blegen N, Peppe DJ. 2020. Late Pleistocene mammals from Kibogo, Kenya: systematic paleontology, paleoenvironments, and non-analog associations. J Vertebr Paleontol. 40:e1841781. doi:10.1080/02724634.2020.1841781.

Faith JT, Tryon CA, Peppe DJ, Beverly E, Blegen N, Blumenthal S, Chritz KL, Driese SG, Patterson D. 2015. Paleoenvironmental context of the middle stone age record from Karungu, Lake Victoria Basin, Kenya, and its implications for human and faunal dispersals. J Hum Evol. 83:28–45. doi:10.1016/j.jhevol.2015.03.004.

Feakins SJ, Levin NE, Liddy HM, Sieracki A, Eglinton TI, Bonnefille R. 2013. Northeast African vegetation change over 12 my. Geology. 41:295–298. doi:10.1130/G33845.1.

Frantz L, Meijaard E, Gongora J, Haile J, Groenen MAM, Larson G. 2016. The evolution of suidae. Annu Rev Anim Biosci. 4:61–85. doi:10.1146/annurev-animal-021815-111155.

Garrett ND, Fox DL, McNulty KP, Faith JT, Peppe DJ, Van Plantinga A, Tryon CA. 2015. Stable isotope paleoecology of Late Pleistocene middle stone age humans from the Lake Victoria basin, Kenya. J Hum Evol. 82:1–14. doi:10.1016/j.jhevol.2014.10.005.

Geraads D, Alemseged Z, Reed D, Wynn J, Roman DC. 2004a. The Pleistocene fauna (other than Primates) from Asbole, lower Awash Valley, Ethiopia, and its environmental and biochronological implications. Geobios Mem Spec. 37:697–718. doi:10.1016/j.geobios.2003.05.011.

Geraads D, Eisenmann V, Petter G 2004b. The large mammal Fauna of the Oldowayan sites of Melka-Kunturé, Ethiopia. Instituto Italiano Di Preistoria E Protoistoria, Studies on the Early Palaeolithic Site of Melka Kunturé. p. 169–192.

Gilbert HW. 2008. Suidae. In: Asfaw GW, editor. *Homo Erectus*: pleistocene evidence from the middle Awash, Ethiopia. Berkeley: University of California Press Berkeley; p. 231–260.

Gongora J, Cuddahee RE, Nascimento FFD, Palgrave CJ, Lowden S, Ho SYW, Simond D, Damayanti CS, White DJ, Tay WT, et al. 2011. Rethinking the evolution of extant sub-Saharan African suids (Suidae, Artiodactyla). Zool Scr. 40:327–335. doi:10.1111/j.1463-6409.2011.00480.x.

Gongora J, Groves C, Meijaard E. 2017. Evolutionary relationships and taxonomy of suidae and tayassuidae. In: Melletti M, Meijaard E, editors. Ecology, conservation and management of wild pigs and peccaries. Cambridge: Cambridge University Press; p. 1–19.

Gray JE. 1821. On the natural arrangement of vertebrose animals. London Medi Repository. 15:296–310.

Groves C, Grubb P. 2011. Ungulate taxonomy. Baltimore: The John Hopkins University Press.

Grubb P. 1993. The Afrotropical suids *Phacochoerus, Hylochoerus*, and *Potamochoerus*. In: Oliver WLR, editor. Pigs, pecaries and hippos. Gland, Switzerland: International Union for Conservation of Nature and Natural Resources (IUCN); p. 66–75.

Grubb P. 2005. Artiodactyla. In: Wilson DE, Reeder DM, editors. Mammal species of the world: a taxonomic and geographic reference. Baltimore: The John Hopkins University Press; p. 637–722.

Harris JM. 1983. Family Suidae. In: Harris JM, editor. Koobi fora research project: volume ii: the fossil ungulates, proboscidea, perissodactyla, and suidae. Oxford: Oxford University Press; p. 215–300.

Harris JM, Brown FH, Leakey MG. 1988. Stratigraphy and paleontology of Pliocene and Pleistocene localities west of Lake Turkana, Kenya. Los Angeles: Natural History Museum of Los Angeles County.

Harris JM, Cerling TE. 2002. Dietary adaptations of extant and Neogene African suids. J Zool. 256:45–54. doi:10.1017/S0952836902000067.

Harris JM, Cerling TE, Leakey MG, Passey BH. 2008. Stable isotope ecology of fossil hippopotamids from the Lake Turkana Basin of East Africa. J Zool. 275:323–331. doi:10.1111/j.1469-7998.2008.00444.x.

Harris JM, White TD. 1979. Evolution of the Plio-Pleistocene African Suidae. Trans American Philos Soc. 69:1–128. doi:10.2307/1006288.

Hendey QB, Cooke HBS. 1985. *Kolpochoerus paiceae* (Mammalia, Suidae) from Skurwerug near Saldanha, South Africa, and its palaeoenvironmental implications. Ann S Afr Mus. 97:9–56.

Janis CM. 1988. An estimation of tooth volume and hypsodonty indices in ungulate mammals, and the correlation of these factors with dietary preferences. Mémoires Du Museum National d'Histoire Naturelle. 53:367–387.

Kingdon J. 1979. East African Mammals: an Atlas of evolution in Africa. Volume III Part B, Large Mammals. London: Academic Press; p. 436.

Lazagabaster IA. 2019. Dental microwear texture analysis of Pliocene Suidae from Hadar and Kanapoi in the context of early hominin dietary breadth expansion. J Hum Evol. 132:80–100. doi:10.1016/j.jhevol.2019.04.010.

Lazagabaster IA, Souron A, Rowan J, Robinson JR, Campisano CJ, Reed KE. 2018. Fossil Suidae (Mammalia, Artiodactyla) from Lee Adoyta, Ledi-Geraru, lower Awash Valley, Ethiopia: implications for late Pliocene turnover and paleoecology. Palaeogeogr Palaeoclimatol Palaeoecol. 504:186–200. doi:10.1016/j.palaeo.2018.05.029.

Leakey LSB. 1942. Fossil Suidae from Oldoway. East African Geog Rev. 1942:178–196.

Lehmann SB, Braun DR, Dennis KJ, Patterson DB, Stynder DD, Bishop LC, Forrest F, Levin NE. 2016. Stable isotopic composition of fossil mammal teeth and environmental change in southwestern South Africa during the Pliocene and Pleistocene. Palaeogeogr Palaeoclimatol Palaeoecol. 457:396–408. doi:10.1016/j.palaeo.2016.04.042.

Lesur J, Faith JT, Bon F, Dessie A, Ménard C, Bruxelles L. 2016. Paleoenvironmental and biogeographic implications of terminal Pleistocene large mammals from the Ziway–Shala Basin, Main Ethiopian Rift, Ethiopia. Palaeogeogr Palaeoclimatol Palaeoecol. 449:567–579. doi:10.1016/j.palaeo.2016.02.053.

Leus K, Macdonald AA. 1997. From babirusa (*Babyrousa babyrussa*) to domestic pig: the nutrition of swine. Proc Nutr Soc. 56:1001–1012. doi:10.1079/PNS19970105.

Linnaeus CV. 1758. Systema naturae per regna tria naturae, secundum classes, ordines, genera, species, cum characteribus, differentiis, synonymis, locis, Tenth edition. Stockholm: Laurentii Salvii, Holmiae; p. 824.

Lüdecke T, Schrenk F, Thiemeyer H, Kullmer O, Bromage TG, Sandrock O, Fiebig J, Mulch A. 2016. Persistent C3 vegetation accompanied Plio-Pleistocene hominin evolution in the Malawi Rift (Chiwondo Beds, Malawi). J Hum Evol. 90:163–175. doi:10.1016/j.jhevol.2015.10.014.

Luyt J, Lee-Thorp JA, Avery G. 2000. New light on middle Pleistocene west coast environments from Elandsfontein, Western Cape Province, South Africa. S Afr J Sci. 96:399–403.

Ma J, Wang Y, Jin C, Hu Y, Bocherens H. 2019. Ecological flexibility and differential survival of Pleistocene *Stegodon orientalis* and *Elephas maximus*

in mainland southeast Asia revealed by stable isotope (C, O) analysis. Quat Sci Rev. 212:33–44. doi:10.1016/j.quascirev.2019.03.021.
Ma J, Wang Y, Jin C, Yan Y, Qu Y, Hu Y. 2017. Isotopic evidence of foraging ecology of Asian elephant (*Elephas maximus*) in South China during the Late Pleistocene. Quat Int. 443:160–167. doi:10.1016/j.quaint.2016.09.043.
Magill CR, Ashley GM, Domínguez-Rodrigo M, Freeman KH. 2016. Dietary options and behavior suggested by plant biomarker evidence in an early human habitat. Proc Natl Acad Sci U S A. 113:2874–2879. doi:10.1073/pnas.1507055113.
Medin T, Martínez-Navarro B, Rivals F, Libsekal Y, Rook L. 2015. The late Early Pleistocene suid remains from the paleoanthropological site of Buia (Eritrea): systematics, biochronology and eco-geographical context. Palaeogeogr Palaeoclimatol Palaeoecol. 431:26–42. doi:10.1016/j.palaeo.2015.04.020.
Melletti M, Breuer T, Huffman BA, Turkalo AK, Mirabile M, Maisels F. 2017. River Hog *Potamochoerus porcus* (Linnaeus, 1758). In: Melletti M, Meijaard E, editors. Ecology, conservation and management of wild pigs and peccaries. Cambridge: Cambridge University Press; p. 134–149.
Negash EW, Alemseged Z, Bobe R, Grine F, Sponheimer M, Wynn JG. 2020. Dietary trends in herbivores from the Shungura Formation, southwestern Ethiopia. Proc Natl Acad Sci U S A. 117:21921–21927. doi:10.1073/pnas.2006982117.
Owen R. 1848. The archetype and homologies of the vertebrate skeleton. London: J. van Voorst; p. 203.
Passey BH, Cerling TE, Levin NE. 2007. Temperature dependence of oxygen isotope acid fractionation for modern and fossil tooth enamels. Rapid Commun Mass Spectrom. 21:2853–2859. doi:10.1002/rcm.3149.
Passey BH, Cerling TE, Perkins ME, Voorhies MR, Harris JM, Tucker ST. 2002. Environmental change in the great plains: an isotopic record from fossil horses. J Geol. 110:123–140. doi:10.1086/338280.
Pearcy RW, Ehleringer J. 1984. Comparative ecophysiology of C3 and C4 plants. Plant Cell Environ. 7:1–13. doi:10.1111/j.1365-3040.1984.tb01194.x.
Potts R, Behrensmeyer AK, Faith JT, Tryon CA, Brooks AS, Yellen JE, Deino AL, Kinyanjui R, Clark JB, Haradon CM, et al. 2018. Environmental dynamics during the onset of the middle stone age in eastern Africa. Science. 360:86–90. doi:10.1126/science.aao2200.
Reyna-Hurtado R, Huart JPD, Turkalo AK. 2017. Forest hog *Hylochoerus meinertzhageni* (Thomas 1904). In: Melletti M, Meijaard E, editors. Ecology, conservation and management of wild pigs and peccaries. Cambridge: Cambridge University Press; p. 114–121.
Rowan J, Faith JT, Gebru Y, Fleagle JG. 2015. Taxonomy and paleoecology of fossil Bovidae (Mammalia, Artiodactyla) from the Kibish Formation, southern Ethiopia: implications for dietary change, biogeography, and the structure of the living bovid faunas of East Africa. Palaeogeogr Palaeoclimatol Palaeoecol. 420:210–222. doi:10.1016/j.palaeo.2014.12.017.
Sage RF, Wedin DA, Li M; Others. 1999. The biogeography of C4 photosynthesis: patterns and controlling factors. C4 Plant Biol. 10:313–376.
Seydack AHW. 2017. Bushpig *Potamochoerus larvatus* (F. Cuvier, 1822). In: Melletti M, Meijaard E, editors. Ecology, conservation and management of wild pigs and peccaries. Cambridge: Cambridge University Press; p. 122–133.
Souron A 2012. Histoire évolutive du genre *Kolpochoerus* (Cetartiodactyla: suidae) au Plio-Pléistocène en Afrique orientale. PhD Thesis, University of Bordeaux.
Souron A. 2017. Diet and ecology of extant and fossil wild pigs. In: Melletti M, Meijaard E, editors. Ecology, conservation and management of wild pigs and peccaries. Cambridge: Cambridge University Press; p. 29–38.
Souron A. 2018. Morphology, diet, and stable carbon isotopes: on the diet of *Theropithecus* and some limits of uniformitarianism in paleoecology. Am J Phys Anthropol. 166:261–267. doi:10.1002/ajpa.23414.
Souron A, Boisserie J-R, White TD. 2015b. A new species of the suid genus *Kolpochoerus* from Ethiopia. Acta Palaeontol Pol. 60:79–96.
Souron A, Merceron G, Blondel C, Brunetière N, Colyn M, Hofman-Kamińska E, Boisserie J-R. 2015a. Three-dimensional dental microwear texture analysis and diet in extant Suidae (Mammalia: cetartiodactyla). Mammalia. 79:279–291. doi:10.1515/mammalia-2014-0023.
Sponheimer M, Lee-Thorp JA. 1999. Oxygen isotopes in enamel carbonate and their ecological significance. J Archaeol Sci. 26:723–728. doi:10.1006/jasc.1998.0388.
Sponheimer M, Lee-Thorp JA. 2001. The oxygen isotope composition of mammalian enamel carbonate from Morea Estate, South Africa. Oecologia. 126:153–157. doi:10.1007/s004420000498.
Suwa G, Souron A, Asfaw B. 2014. Fossil Suidae of the Konso formation. Konso-Gardula Res Project. 1:73–88.
Thenius E. 1981. Zur stammesgeschichtlichen Herkunft von *Hylochoerus meinertzhageni* Thomas (Suidae, Mammalia). Zeitschrift Für Säugetierkunde. 46:108–122.
Thomas O. 1904. On *Hylochoerus*, the forest-pig of central Africa. Proc Zool Soc London II. 74:193–199.
Tryon CA, Faith JT, Peppe DJ, Beverly EJ, Blegen N, Blumenthal SA, Chritz KL, Driese SG, Patterson D, Sharp WD. 2016. The Pleistocene prehistory of the Lake Victoria basin. Quat Int. 404:100–114. doi:10.1016/j.quaint.2015.11.073.
Tryon CA, Faith JT, Peppe DJ, Fox DL, McNulty KP, Jenkins K, Dunsworth H, Harcourt-Smith W. 2010. The Pleistocene archaeology and environments of the Wasiriya beds, Rusinga Island, Kenya. J Hum Evol. 59:657–671. doi:10.1016/j.jhevol.2010.07.020.
Tryon CA, Peppe DJ, Faith TJ, Van Plantinga A, Nightingale S, Ogondo J, Fox DL. 2012. Late Pleistocene artefacts and fauna from Rusinga and Mfangano islands, Lake Victoria, Kenya. Azania: Archaeological Research in Africa. 47:14–38. doi:10.1080/0067270X.2011.647946.
Uno KT, Cerling TE, Harris JM, Kunimatsu Y, Leakey MG, Nakatsukasa M, Nakaya H. 2011. Late Miocene to Pliocene carbon isotope record of differential diet change among east African herbivores. Proc Natl Acad Sci U S A. 108:6509–6514. doi:10.1073/pnas.1018435108.
White TD. 1995. African omnivores: global climatic change and Plio-Pleistocene hominids and suids. In: Vrba ES, Denton G, editors. Paleoclimate and evolution, with emphasis on human origins. New Haven: Yale University Press; p. 369–384.
White TD, Ambrose SH, Suwa G, Su DF, DeGusta D, Bernor RL, Boisserie J-R, Brunet M, Delson E, Frost S, et al. 2009. Macrovertebrate paleontology and the pliocene habitat of ardipithecus ramidus. Science. 326:87–93. doi:10.1126/science.1175822.
Yakir D. 1998. Oxygen-18 of leaf water: a crossroad for plant-associated isotopic signals. In: Griffiths H, editor. Stable Isotopes: integration of biological, ecological and geochemical processes. London: Garland Science; p. 147–168.